JOURNAL OF MATERIALS SCIENCE **35** (2000) 2481–2491

Fracture and yield behavior of adhesively bonded joints under triaxial stress conditions

M. IMANAKA*
Department of Technology Education, Osaka University of Education, Asahigaoka, Kashiwara City, Osaka, 582-8582, Japan
E-mail: imanaka@cc.osaka-kyoiku.ac.jp

A. FUJINAMI
Department of Mechanical Engineering, Osaka City University, Sugimoto-cho, Sumiyoshi-ku, Osaka,558-8585, Japan

Y. SUZUKI
Nippon Sharyo, Ltd., 1-1 Sanbonmatsu-hco, Atsuta-ku, Nagoya, 456-8691, Japan

Most of adhesively bonded joints are under complicatedly distributed triaxial stress in the adhesive layer. For the estimating of the strength of adhesively bonded joints, it is crucial to clarify behavior of yield and failure of the adhesives layer under triaxial stress conditions. Two types of the adhesively bonded joints were used in this study: One is the scarf joint which is under considerably uniform normal and shear stresses in the adhesive layer, where their combination ratio can be varied with scarf angle. The other is the butt joint with thin wall tube in which considerably uniform pure shear can be realized in the adhesive layer under torsional load conditions. These joints can cover the stress triaxiality in adhesive layers of most joints in industrial application. The effect of stress triaxiality on the yield and fracture stresses in the adhesive layer were investigated using the joints bonded by three kinds of adhesives in heterogeneous and homogeneous systems. The results showed that both the yield and failure criterion depend on the stress triaxiality and that the fracture mechanism of the homogeneous adhesive is different from that of the heterogeneous one. From these experimental results, a method of estimating the yield and failure stresses was proposed in terms of a stress triaxiality parameter.

1. Introduction

In the stress analysis of adhesively bonded joints, the adhesive layer is usually treated as an elastic body. Recently the ductility of structural adhesives has been improved drastically, which requires the elasto-plastic analysis of the adhesive layer. For the elasto-plastic analysis of adhesively bonded joints, in general, yield condition of the adhesive layer is assumed to be the same as that of bulk adhesive specimen under uniaxial loading; however, it is difficult to think that experiences the same condition because most adhesively bonded joints are under complicatedly distributed triaxial stress in the adhesive layer.

Recently, the yield behavior of polymeric materials has been investigated under biaxial tensile loading and under hydrostatic pressure [1–4]. In the practical situation, the adhesive layer is imposed stress triaxiality of biaxial tensile and uniaxial compression loading or triaxial tensile loading [5]. Hence, the yield criteria of bulk adhesives obtained from these tests cannot simply apply to the estimation of yield behavior of the adhesive layer. In such triaxial stress conditions appearing in the adhesive layer, the characteristics of yield and fracture have not been reported even for the bulk polymeric materials from difficulty in testing.

Adhesively bonded butt and scarf joints provide considerably uniform stress distribution in the adhesive layer except in the vicinity of the free end, and their stress triaxiality varies extensively depending on the scarf angle [6–9]. However, pure shear stress cannot be provided in the adhesive layer of the scarf joints but of the butt joint with thin wall tube under torsional loading [10].

To elucidate the effect of stress triaxiality in the adhesive layer on the yield and fracture, the present study was made of tensile and torsional tests for scarf joints with various scarf angles and the butt joints with thin wall tube respectively, where three kinds of adhesives having different ductility were used. In the tests, the stress triaxiality in the adhesive layer can be realized under conditions from pure shear to triaxial tension, which covers the stress triaxiality of most joints for industrial use. Based on the experimental results, we will demonstrate that yield and fracture conditions for the

* Author to whom all correspondence should be addressed.

TABLE I Mix proportions and curing conditions of the adhesives

Name	System	Formulation of adhesive (gr)	Curing conditions
Unmodified adhesive	Homogeneus system	• Epoxy resin 20 (Asahidenka-kogyo : EP4100E) • Piperiding 1	20 h at 373 K
Thiokol-modified adhesive	Homogeneous system	• Epoxy resin 20 • Piperidine 1.5 • Thiokol (LP-3) 10	20 h at 373 K
Rubber-modified adhesive	Heterogeneous system	• Rubber-modified 25 epoxy resin (Japan Synthesis Rubber : XER91) • Piperidine 0.8	5 h at 433 K

adhesive joints can be evaluated in terms of a stress triaxiality parameter in the adhesive layer.

2. Experimental procedure

2.1. Adhesives, adherend and adhesive joints

The composition and curing conditions of three kinds of epoxy-based adhesives used in this study are given in Table I: unmodified, thiokol-modified and rubber-modified adhesives. The unmodified adhesive was cured from the epoxy resin (Asahi Denka Kogyo, EP4100E) by piperidine, then its adhesive layer showed a little yielding behavior. To improve the ductility of the unmodified adhesive, thiokol (Toray, LP-3) was used as a plasticizer. The two adhesives are of homogeneous system. The rubber-modified adhesive is of heterogeneous system in which rubber particles of 70 nm in average diameter were dispersed. The mixing of each adhesive was carried out under the pressure of 10 mm Torr or less for removing gas bubbles.

Fig. 1 shows the shape and dimension of a scarf joint. Low carbon steel (JIS. SS400) was used as the adherend whose thickness was varied to keep a constant adhesion area. The scarf angle θ was varied from 15° to 90° (butt joint) every fifteen degrees. Fig. 2 is that of a butt joint with thin wall tube whose adherend was structural carbon steel (JIS. S45C). The adhesive layer thickness of all the joints was adjusted to 0.3 mm. The bonding surface of adherends was polished with an emery paper of 320 mesh under dry conditions, then, cleaned with acetone in a ultrasonic bath.

Both the tensile and compression tests for each bulk adhesive were also conducted using dumbbell type (JIS. K7113) and cylindrical type (JIS. K7208) specimens, respectively.

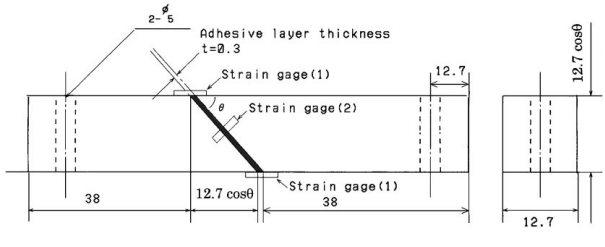

Figure 1 Shape and sizes of the scarf joints.

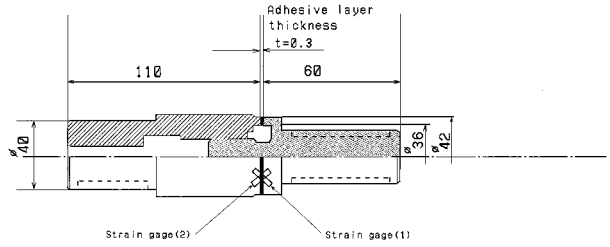

Figure 2 Shape and sizes of the butt joint with thin wall tube.

2.2. Procedure of tensile, compression and torsional tests

For the scarf joints and bulk adhesive specimens both the tensile and compression tests were carried out with a universal testing machine (Shimadzu: Autograph DCS-5000) at the 1 mm/min crosshead speed. In the measurement of strain of the bulk adhesives, a differential transformer was used for the tensile test; a strain gauge was pasted on the test piece for the compression test. To obtain Poisson's ratios of the bulk adhesives, strains in the longitudinal and lateral directions were measured in a elastic range of tensile specimens using two directional strain gages. Strain of the scarf joints was measured by use of strain gauge (1) and (2) in Fig. 1, which were pasted in the loading direction and normal one to the adhesive/adherend interface across the adhesive layer, respectively.

For the butt joint with thin wall tube the torsional tests of were conducted using a torque-controlled torsional testing machine (50 Nm in capacity) at the torsional load speed 27 Nm/min. Strain of the butt joint with thin wall tube was also measured using the two strain gages (1) and (2) pasted on the adhesive layer with the angle of ±45° to the adhesive layer as shown in Fig. 2. All the tests were carried out in a chamber adjusted at 295 ±1 K and below 50% relative humidity.

2.3. Stress and strain of the adhesive joints

On the scarf joint, outputs from the strain gauge (1) and (2) in Fig. 1 involve the strain of the adherend; hence, it is necessary to obtain net strains in the adhesive layer ε_0 and ε_n in Fig. 3. Here the gage outputs were corrected for the adhesive layer thickness, assuming that Young's modulus of the adherend is 210 GPa. Fig. 3 illustrates the simplification of stresses and strains of the scarf joint, in which the z- and s-directions, ε_z and ε_s, are zero from to the constraint of the adherend. When the strains in the three directions on the identical plane, ε_0, ε_n and ε_s are known, the principal strains can be obtained by solving the following equations [11].

$$\varepsilon_0 = \frac{\varepsilon_1 + \varepsilon_3}{2} + \frac{\varepsilon_1 - \varepsilon_3}{2}\cos\alpha \tag{1}$$

$$\varepsilon_s = \frac{\varepsilon_1 + \varepsilon_3}{2} + \frac{\varepsilon_1 - \varepsilon_3}{2}\cos 2(\alpha - \vartheta) \tag{2}$$

$$\varepsilon_n = \frac{\varepsilon_1 + \varepsilon_3}{2} + \frac{\varepsilon_1 - \varepsilon_3}{2}\cos\left(\alpha + \frac{\pi}{2} - \vartheta\right) \tag{3}$$

where ε_1 and ε_3 are the minimum and the maximum principal strains, respectively, α is the angle between

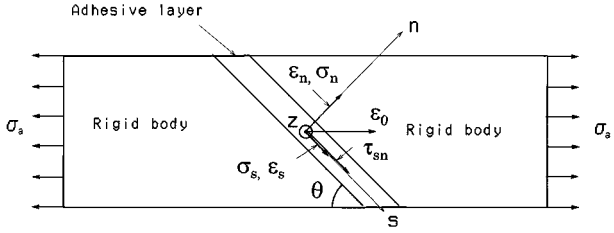

Figure 3 Simplification of stress and strains of the scarf joint in the adhesive layer.

the maximum principal strain and loading directions, and θ is the scarf angle.

Scarf joints have considerably uniform stress distributions in the adhesive layer except the vicinity of the free end [7]. As Fig. 3 shows, the normal stress, σ_n, and shear stress, τ_{sn}, are given in the uniform stress region as follows [6]:

$$\sigma_n = \sigma_a \sin^2\theta \tag{4}$$

$$\tau_{sn} = \sigma_a \sin\theta \cos\theta \tag{5}$$

where σ_a is the average axial stress. In addition, since ε_s and ε_z are zero as mentioned above, when both the adhesive and adherend are assumed as a elastic body under plane strain condition, the s and z directional stresses σ_s, and σ_z are given by.

$$\sigma_s = \sigma_z = \frac{\sigma_n \nu_a}{(1-\nu_a)} \tag{6}$$

where ν_a is Poisson's ratio of the adhesive layer. Using Equations 4–6, the maximum principal stress, σ_1, can be obtained as.

$$\sigma_1 = \frac{1}{2}\{\sigma_s + \sigma_n + \sqrt{(\sigma_s - \sigma_n)^2 + 4\tau_{sn}} \tag{7}$$

Hereafter, we will discuss the stress-strain curves of the adhesion layer are shown using the maximum principal stress and the maximum principal strain. The maximum shear stress of the butt joint of thin wall tube was obtained from the following equation [10].

$$\tau_{max} = \frac{16 d_2 T}{\pi\left(d_2^4 - d_1^4\right)} \tag{8}$$

where d_1 and d_2 are the inner and outer diameters, respectively, and T is the applied torque. The strain of the adhesive layer was calculated from the output of the two strain gages pasted on the adhesive layer. Here the maximum shear stress being obtained from the equation [12].

$$\gamma_{max} = \frac{\sqrt{2}}{\eta}\left\{\varepsilon_s L_g - (L_g - \sqrt{2}\eta)\frac{8 t d_2}{G_a \pi\left(d_2^4 - d_1^4\right)}\right\} \tag{9}$$

where η is adhesive layer thickness, ε_s is the average value of the strains from the two gages, L_g the gage length, and G_a the shear modulus of the adherend which was assumed to be 76 GPa.

3. Results and discussion

3.1. Stress-strain curves of the bulk adhesive

Thiokol is widely used as a plasticizer which improves flexibility and impact resistance of epoxy resin [13]; however, it leads to reduction of the static strength from softening the resin itself. Recently, the rubber modified epoxy adhesives containing dispersed rubber particles used for structural bonding, because of making extensive improvement in the fracture toughness, though reducing the static strength a little [14].

Figs 4 and 5 show the stress-strain curves of the three bulk adhesive specimens under tensile and compression load conditions, respectively, wherein engineering stress was modified with the elongation assuming that the test specimen was uniformly deformed, and the resultant stress is given as the ordinate. As Fig. 4 shows, the unmodified adhesive exhibits a little yield behavior.

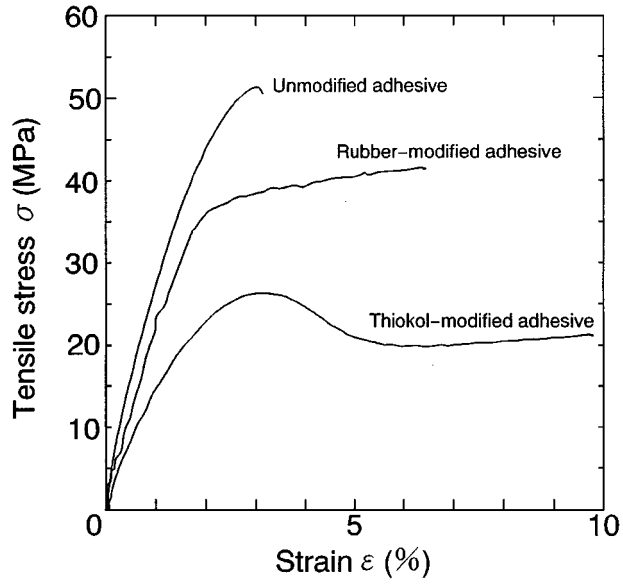

Figure 4 Stress-strain curves for the bulk adhesives under tensile load condition.

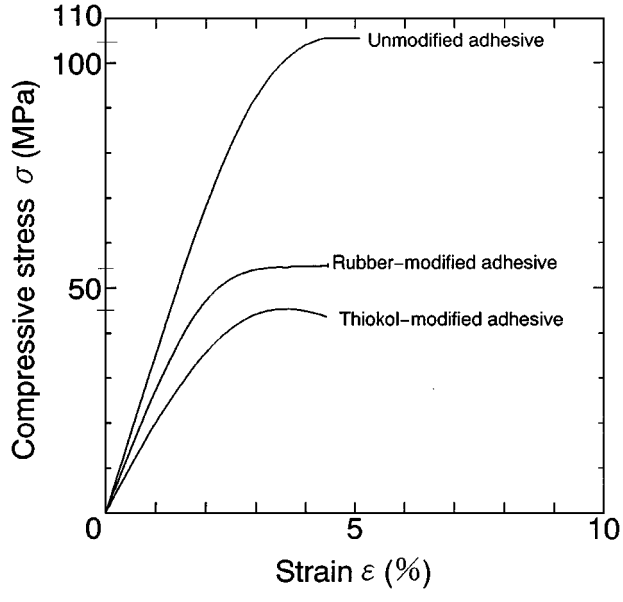

Figure 5 Stress-strain curves for the bulk adhesives under compression load condition.

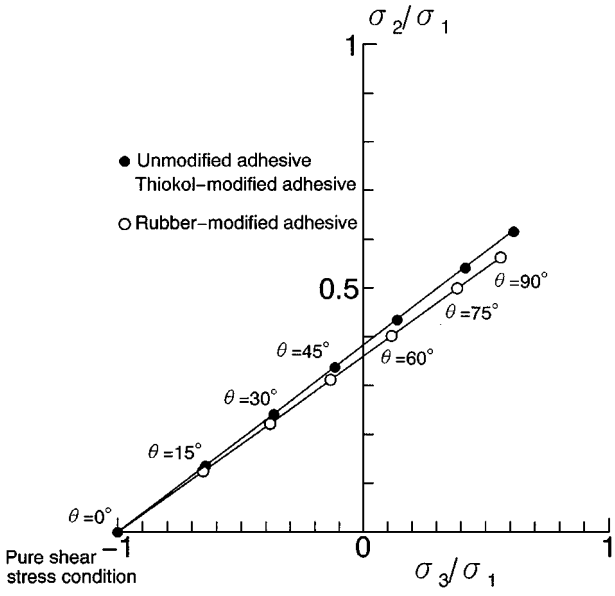

Figure 6 Stress triaxility in the adhesive layer.

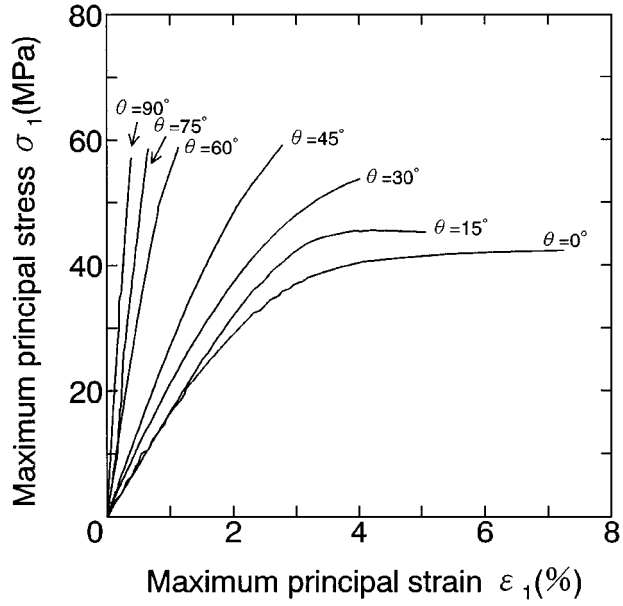

Figure 7 Stress-strain curves for scarf joints and butt joint with thin wall tube (Unmodified adhesive).

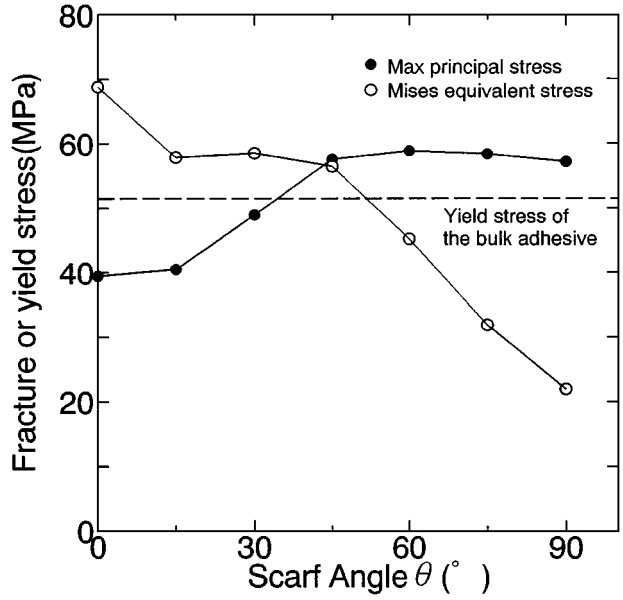

Figure 8 Effect of scarf angle on fracture or yield stress (Unmodified adhesive).

Whereas thiokol-modified adhesive dose clear yield behavior and give rise to neck after passing through a maximum stress. Comparing stress-strain curve of the unmodified adhesive with that of thiokol-modified adhesive, it is observed that the strength and rigidity of the latter are considerably lower than those of the former. For the rubber modified adhesive, although yield behavior is clearly observed, the modulus of elasticity is almost equivalent to the unmodified adhesive and the breaking strength is about 80% of that for the unmodified adhesive. Besides, stress whitening phenomenon was observed, which may be damaged by the occurrence of micro-voids [14]. From these observations, it can be concluded that the stress-strain behavior of the rubber- and thiokol-modified adhesives is similar to each other in general tendency as mentioned above [13, 14].

Fig. 5 shows the stress-strain curves of the bulk adhesives under compression loading. Yield behavior is observed for all the adhesives, but stress whitening was not observed for the rubber modified adhesive. This indicates that stress whitening depends on loading conditions. Moreover, the compressive strength is 1.5–2 times as high as the tensile strength irrespective of a kind of the adhesives; such tendency is in general characteristic of the many polymeric materials [15].

TABLE II Mechanical properties of the bulk adhesives

	Yield stress σ_y (MPa)		Young's modulus E_a (GPa)	Poisson's ratio ν_a
	Tensile loading	Compression loading		
Unmodified adhesive	51	104.7	2.86	0.38
Thikol modified adhesive	26.5	54.5	1.17	0.38
Rubber modified adhesive	37.7	45.0	2.02	0.36

The mechanical properties of the bulk adhesives are summarized in Table II. The yield stress was defined as the stress at the peak or at the intersection of the initial slope with the final slope of the stress-strain curves in Figs 4 and 5 [15].

3.2. Stress triaxiality in the adhesive layer

Generally, the ductility of most polymeric materials depends on stress triaxiality [15]. For the all adhesively bonded joints in this study to elucidate the stress triaxiality in the adhesive layer, the principal stress ratios in the uniform stress region are shown in Fig. 6 as a plots of σ_3/σ_1 against σ_2/σ_1, where σ_1 is the maximum principal stress, σ_2 and σ_3 are the medium principal stress and the minimum principal stress, respectively. In the present situation, since the plane strain condition was assumed, the stress triaxiality

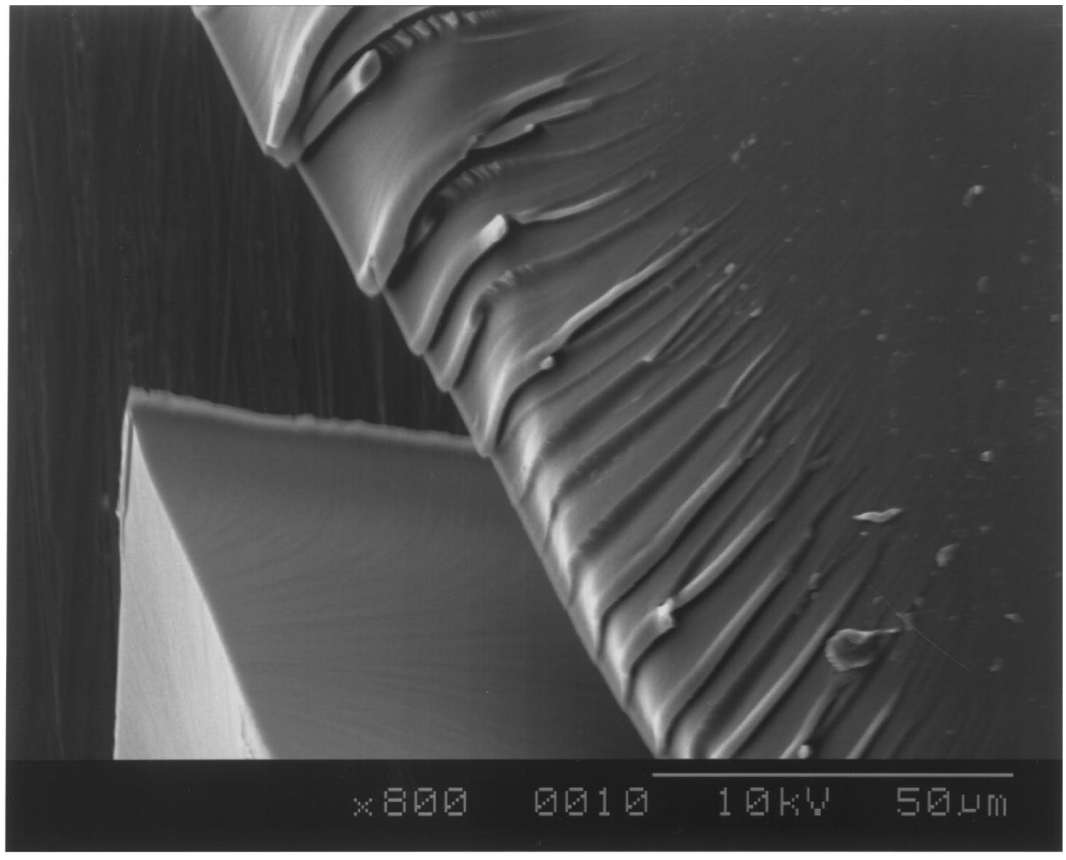

(a) $\theta = 15°$

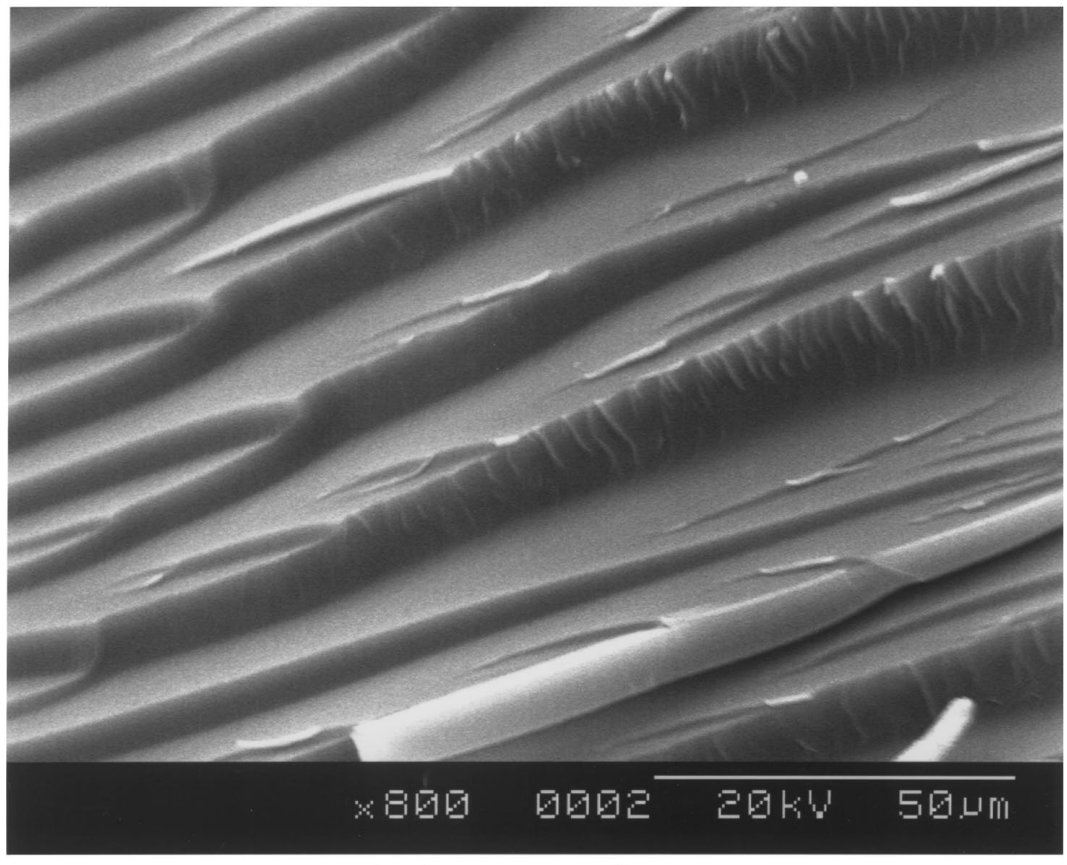

(b) $\theta = 60°$

Figure 9 Examples of fracture surface of scarf joint (Unmodified adhesive).

TABLE III Fracture morphology of the adhesively bonded joints

Adhesive	Scarf angle θ	Fracture surfaces obtained from SEM	Fracture appearances obtained from stress-strain curves
Unmodified adhesive	15°	Slip	Ductile
	30°	Slip	Ductile
	45°	Slip	Ductile
	60°	Cleavage step	Brittle
	75°	Cleavage step	Brittle
	90°	Cleavage step	Brittle
Thiokol-modified adhesive	15°	Slip	Ductile
	30°	Slip	Ductile
	45°	Slip	Ductile
	60°	Slip	Ductile
	75°	Slip	Ductile
	90°	Cleavage step	Brittle
Rubber-modified adhesive	15°	Shear dimple	Ductile
	30°	Shear dimple	Ductile
	45°	Shear dimple	Ductile
	60°	Equiaxed dimple	Ductile
	75°	Equiaxed dimple	Ductile
	90°	Equiaxed dimple	Ductile

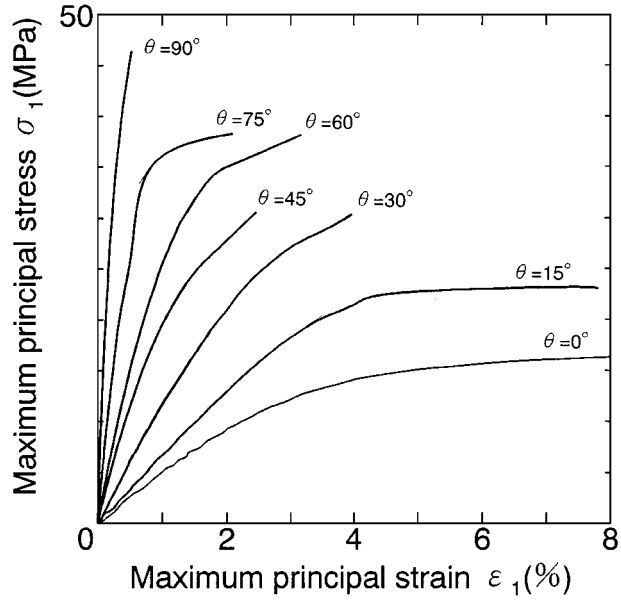

Figure 10 Stress-strain curves for scarf joints and butt joint with thin wall tube (Thiokol-modified adhesive).

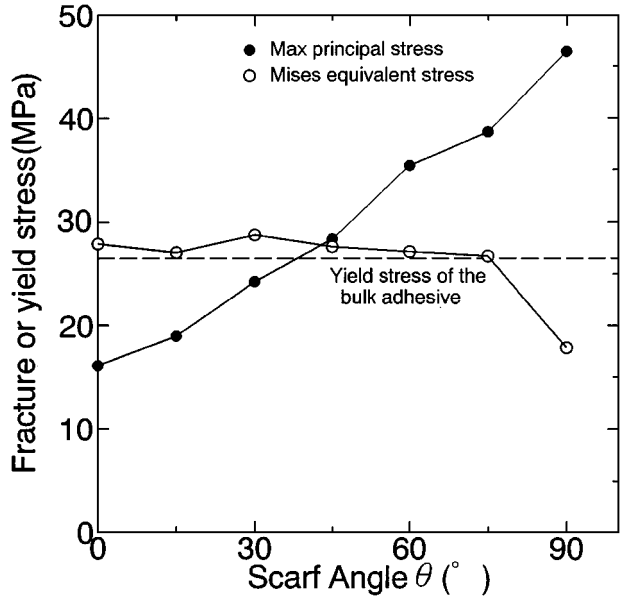

Figure 11 Effect of scarf angle on fracture or yield stress (Thiokol-modified adhesive).

can be defined by only one parameter of either σ_3/σ_1 or σ_2/σ_1. In addition, a following linear relationship exists between σ_3/σ_1 and σ_2/σ_1 [5]

$$\frac{\sigma_2}{\sigma_1} = \nu_a + \nu_a \frac{\sigma_3}{\sigma_1} \tag{10}$$

This equation indicates that the triaxiality in the adhesive layer can only be determined by the Poisson's ratio of the adhesive layer, ν_a. This figure indicates that the stress triaxiality increases with increasing in the scarf angle, and that the stress conditions are under biaxial tension and uniaxial compression in the range of $\theta \leq 45°$, and under triaxial tension for $\theta \geq 60°$.

3.3. Strength characteristics of the joints bonded by the unmodified adhesive

Fig. 7 shows the stress-strain curves in the adhesive layer for the scarf joints and butt joint with thin wall tube bonded by the unmodified adhesive, which represents the relationship between the maximum principal stress and the maximum principal strain of the adhesion layer. The stress-strain curve in the torsion test is given as $\theta = 0°$, since the stress state in the adhesive layer under torsional loading corresponds to that of the scarf joint with $\theta = 0°$. In the figure, brittle fracture occurred at the scarf angle $\theta = 60°$, 75°, 90°, and yield behavior is observed at the scarf angle $\theta = 15°$, 30°, 45°, and in the torsional test ($\theta = 0°$).

In the tensile test of scarf joints bonded with another epoxy adhesives, it has been reported from that the yield of the adhesive layer is governed by the Mises equivalent stress and brittle fracture is done by the maximum principal stress [8]. Fig. 8 shows the relationship between the scarf angle and the maximum principal stress at the fracture point or Mises equivalent stress at the yield point in the adhesive layer which was determined from the intersection of the initial slope with the final one of the stress-strain curve [15]. In the figure, the yield stress of the bulk adhesive specimen is also indicated as a dashed line. The maximum principal stresses for the scarf joints with $\theta = 60°$–90° and the Mises equivalent stress for the joints with $\theta = 15°$–45° are almost the same at the fracture and yield points, respectively, where brittle fracture occurred in the former joints and yield behavior appeared in the latter joints. Such trend agree with the trend in the previous paper as mentioned above [8]. In Fig. 8 the yield stress for the joints with $\theta = 15°$–45° is greater than that of the bulk specimen by a factor of 12%. This may be due to the volume effect of the adhesive, because this adhesive is sensitive to the defect.

Fig. 9a and b show typical photos of fracture surface of the scarf joints with $\theta = 15°$ and 60° on a scanning electron microscope. As shown in Fig. 9a, in case of $\theta = 15°$, slip plane destruction in the layer structure is

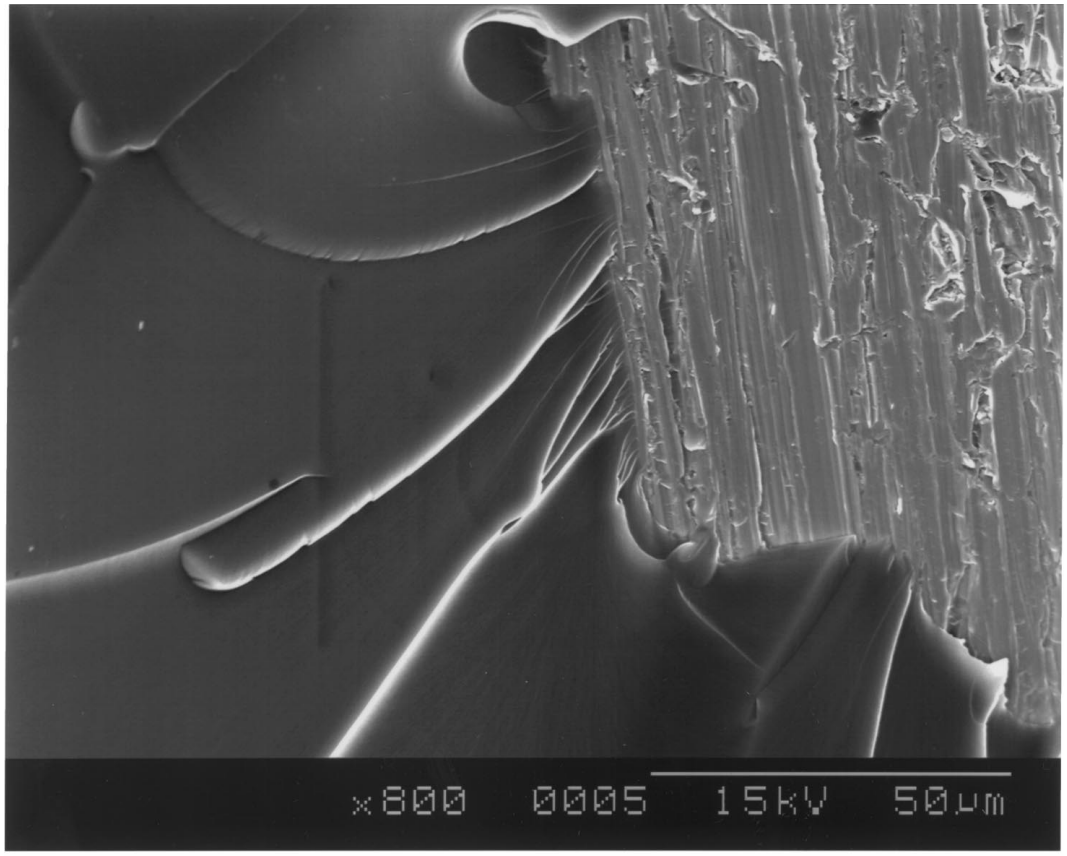

(a) $\theta = 15°$

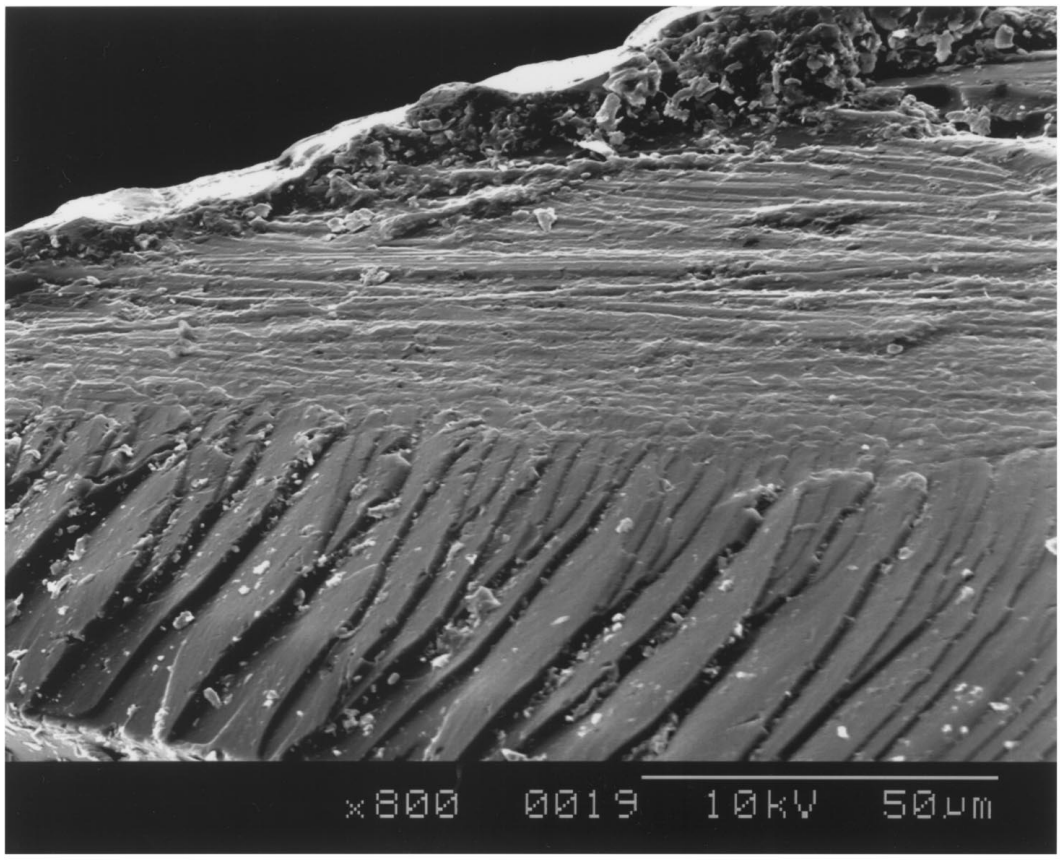

(b) $\theta = 90°$

Figure 12 Examples of fracture surface of scarf joint (Thiokol-modified adhesive).

observed, which shows a typical ductile fracture pattern. For $\theta = 60^\circ$ as shown in Fig. 9b, the cleavage step state is observed, which is a typical brittle fracture pattern [16].

3.4. Strength characteristics of the joints bonded by the thiokol-modified adhesive

Fig. 10 shows the stress-strain curves of the scarf joints and butt joint with thin wall tube bonded by the thiokol modified adhesive. For all the joints except the butt joint with $\theta = 90^\circ$ yield behavior is observed. Transition scarf angle θ at which the fracture pattern changes ductile to brittle is between 75° and 90°, being higher than that of the unmodified adhesive. This is because the ductility of the adhesive was improved by the thiokol-modification. The relationship between the scarf angle and fracture or yield stress is given in Fig. 11. The Mises equivalent stresses at yield point provide almost constant value in the range of $0^\circ \leq \theta \leq 75^\circ$. This indicates that the yield stress of ductile fracture and the breaking stress of brittle fracture for the both unmodified and thiokol-modified adhesives can be standardized in terms of the Mises equivalent and the maximum principal stress, respectively. In addition, the Mises equivalent stress at the yield point almost agrees with that of the bulk adhesive specimen. This is attributable to that the thiokol-modification reduces the sensibility of fracture to the defect in the adhesive layer.

Fig. 12 shows the fracture surfaces for the joints with scarf angle $\theta = 15^\circ$ and 90° with a scanning electron microscope. For the joint at $\theta = 15^\circ$, slip plane destruction in layer structure is found and these extended layers overlap. This implies the generation of large-scale deformation compared to the fracture surface of the unmodified adhesive. On the fracture surface for $\theta = 90^\circ$, the cleavage step as typical pattern of the brittle fracture is observed. Table III shows the morphology of the fracture surfaces of the scarf joints. For both the unmodified and thiokol-modified adhesives, the transition angle from ductile fracture to brittle fracture agrees with that of fracture pattern from slip to cleave step.

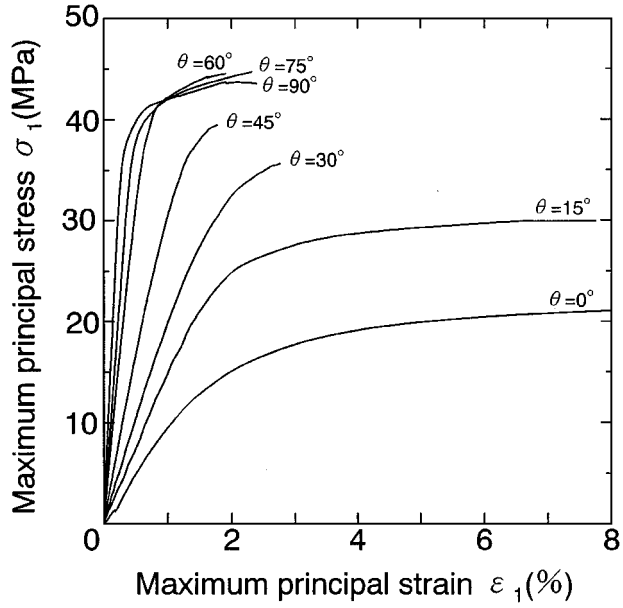

Figure 13 Stress-strain curves for scarf joints and butt joint with thin wall tube (Rubber-modified adhesive).

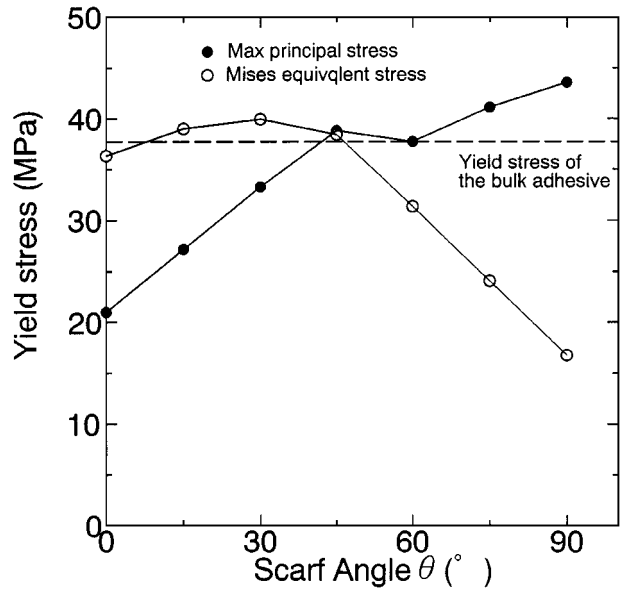

Figure 14 Effect of scarf angle on fracture or yield stress (Rubber-modified adhesive).

3.5. Strength characteristics of the joints bonded by the rubber modified adhesive

Fig. 13 shows the stress-strain curves of the scarf joints and butt joint with thin wall. All the joints exhibit yielding behavior. In the same way as the unmodified and thiokol modified adhesive, the relationship between the scarf angle and the yield stress was obtained as Fig. 14. The Mises equivalent stress at the yield point is almost constant in the range of $0^\circ \leq \theta \leq 45^\circ$, and the maximum principal stress at the yield point somewhat increases with the scarf angle for $60^\circ \leq \theta \leq 90^\circ$.

For the butt joint ($\theta = 90^\circ$), shear deformation of the adhesive layer cannot occur except in the vicinity of the end of the adhesive layer. Therefore, the fracture mechanism for the joints of $\theta \leq 45^\circ$ will be expected to differ from that of the joints in $60^\circ \leq \theta \leq 90^\circ$. Recently, a fracture mechanism of rubber-modified epoxy resin under plane strain condition has been proposed [17]: At first, cavitation occurs surroundings of the rubber particle; then stress state of the inside of the matrix resin changes from the plane strain condition into the plane stress condition where the stress triaxiality of the matrix resin weakens. This is because yielding of the adhesive layer occurs even in the butt joint.

Stress whitening was also observed for the rubber-modified bulk specimen under tensile loading. Hence, it is expected that the cavitation also occurs in the adhesive layer: for the joints in $60^\circ \leq \theta \leq 90^\circ$, cavitation surrounding the rubber particles occurs from the expansion stress, which makes yielding in the adhesive layer similar to the bulk matrix resin as mentioned above. In addition, the maximum principal stress at the yield point agrees with the yield stress of the bulk adhesive

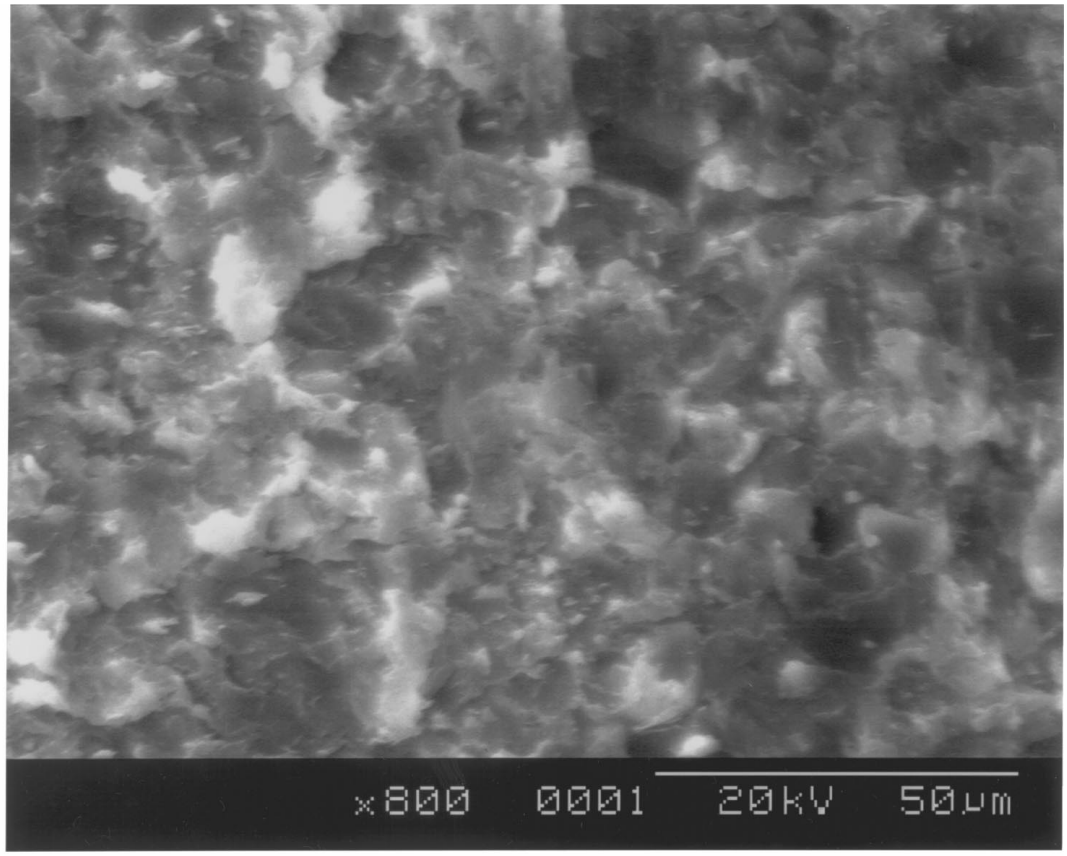

(a) $\theta = 15^\circ$

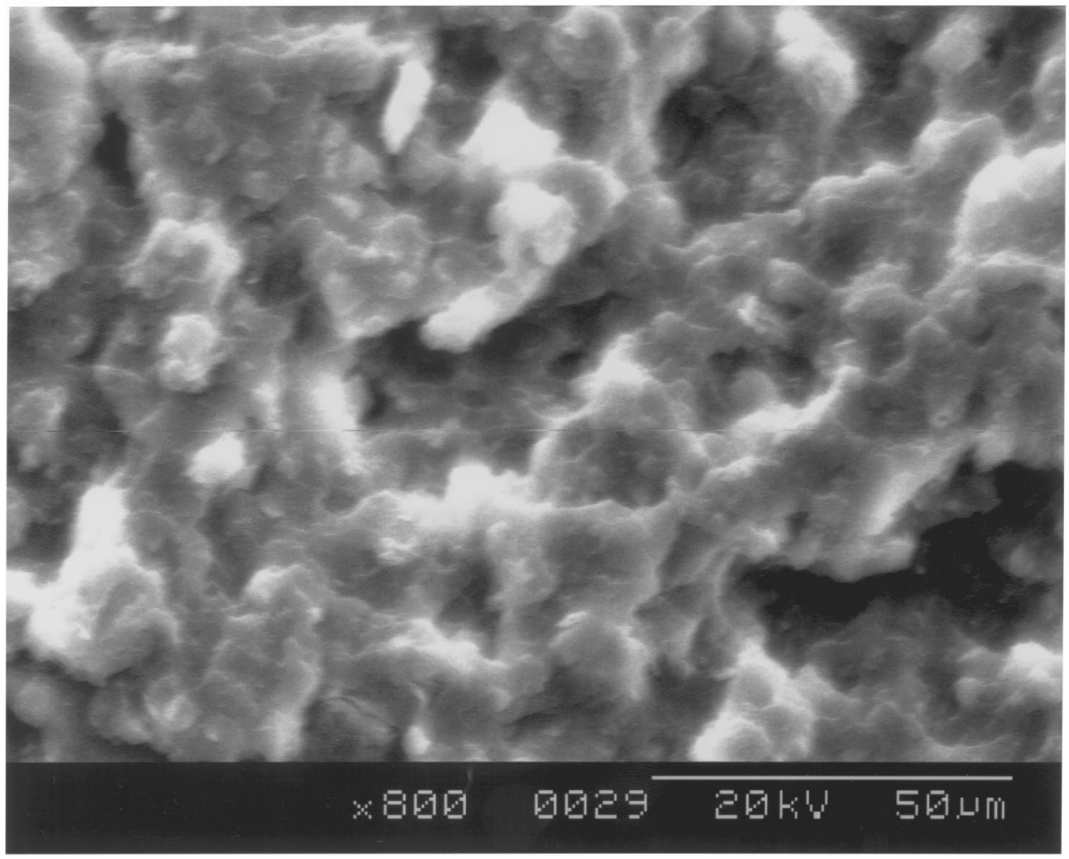

(b) $\theta = 90^\circ$

Figure 15 Examples of fracture surface of scarf joint (Rubber-modified adhesive).

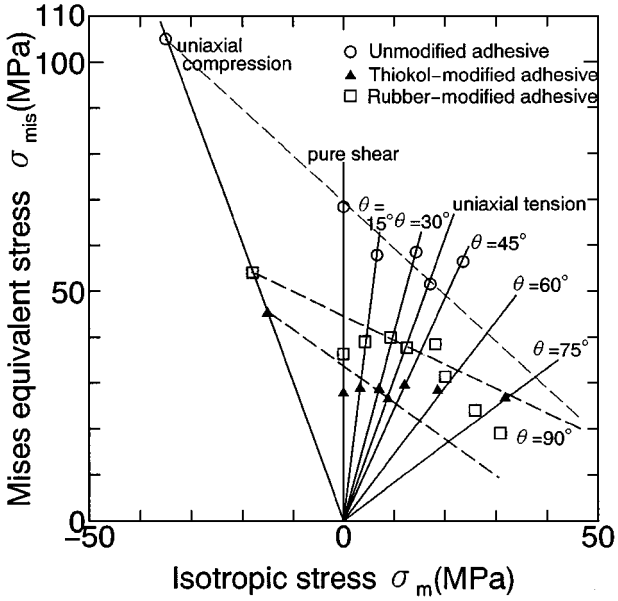

Figure 16 Relation between the mean hydrostatic stress and the Mises equivalent stress.

specimen under tensile loading, where stress state of the bulk specimen is under the plane stress condition. This suggests that for the scarf joints of $60° \leq \theta \leq 90°$ the stress state in the adhesive layer changes from plane strain condition into plane stress condition with increasing applied load.

For the joints of $\theta \leq 45°$, the Mises equivalent stress at the yield point is almost constant irrespective of the scarf angles. This suggests that shear yielding occurs in the adhesive layer.

Fig. 15 shows fracture surfaces of the joint of $\theta = 15°$ and $90°$. Shear dimple was observed in Fig. 15a of $\theta = 15°$, implying that plastic deformation by the sliding may occur. Equiaxed dimple was observed in Fig. 15b of $\theta = 90°$. Both fracture surfaces of $\theta = 15°$ and $\theta = 90°$ are typical ductile fracture surfaces [18]; in addition, transition angle of the fracture surface form shear dimple to equiaxed dimple is between 45° and 60° (see Table III), corresponding to the transition angle from shear yielding to damage yielding.

3.6. Effect of mean hydrostatic stress on the yield stress

Hydrostatic pressure affects the yield stress of most polymeric materials [15]; hence, the effect of positive average hydrostatic pressure on the yield stress has been investigated. The yield condition is usually evaluated by a modified Mises equation involving the term of the mean hydrostatic pressure [1–4]. However, yield and fracture behavior in the triaxial stress state appearing in many adhesively bonded joints have been rarely investigated.

Fig. 16 shows the relation between the mean hydrostatic pressure and the yield stress in the adhesion layer, in which the results of tensile and compression tests for the bulk adhesive specimens are also indicated. Dolve *et al.* conducted the torsional tests of butt joint with thin wall tube as well as the tensile and compression

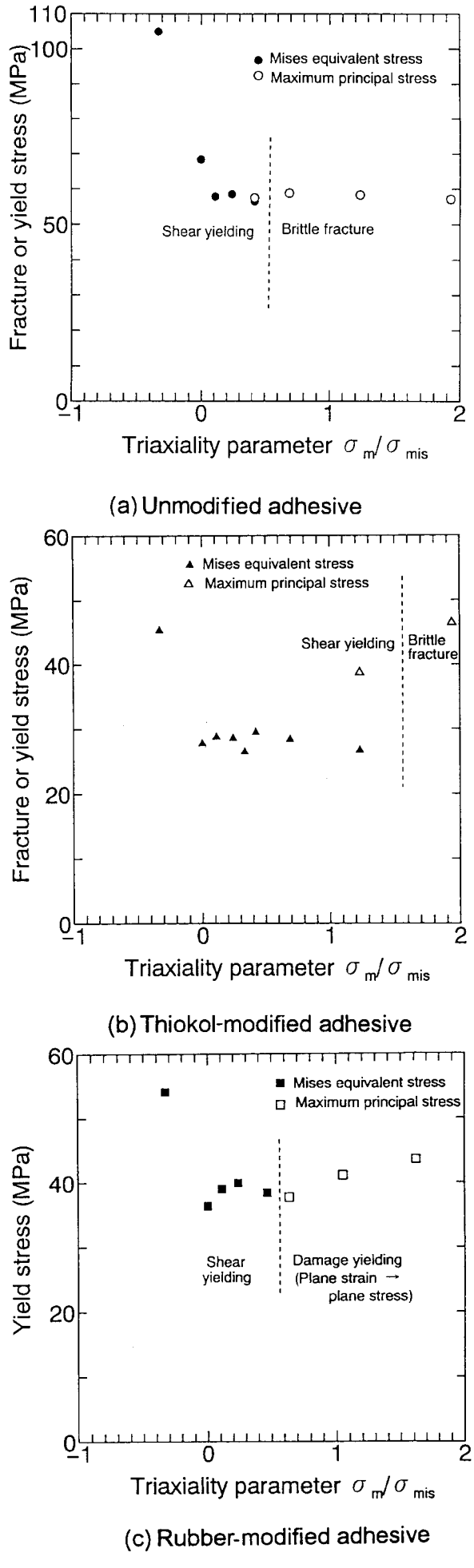

Figure 17 Effect of stress multiaxiality on fracture or yield stress.

tests for the bulk adhesive specimens. They found that a linear relationship exists between the Mises equivalent stress and the mean stress [19]. This means that the yield stress can be evaluated by the modified Mises equation. Hence, to clarify the linear relationship, the dashed lines connecting yield stresses obtained from the uniaxial tension and compression tests are compared with the joint data. As Fig. 16 shows, yield stress in the range of $\sigma_m \leq 0$ increases with increasing hydrostatic stress for all the adhesives used in this work. This trend is similar to that of the modified Mises equation. However, when $\sigma_m > 0$, for the unmodified and the thiokol-modified adhesives the Mises equivalent stress dose not vary significantly with the mean hydrostatic stress. Whereas, for the rubber-modified adhesive, it is observed that the Mises equivalent stress decreases with increasing the mean hydrostatic pressure in the range of $60^\circ \leq \theta \leq 90^\circ$. In the range of $0^\circ \leq \theta \leq 45^\circ$, the Mises equivalent stress is almost constant in the same manner as the unmodified and thiokol-modified adhesives.

From the above-mentioned results, it can be concluded that the modified Mises equation is not applicable to the yield criteria of the adhesives.

3.7. Evaluation of yield and fracture stresses with the stress triaxiality parameter

Even for the same stress triaxiality, the mean hydrostatic pressure varies with strength of the adhesive; thus the mean stress is not suitable for a parameter representing the stress triaxiality in the adhesive layer. As a parameter for the stress triaxiality, σ_m/σ_{mis} was examined in this study, where σ_m is the mean stress and σ_{mis} is the Mises equivalent stress [20].

Yield and fracture stresses were evaluated from the stress triaxiality parameter. The results are shown in Fig. 17, where the value on the ordinate indicates the Mises equivalent stress at yield point or the maximum principal stress at the fracture point, the value on the abscissa doing the stress triaxiality parameter σ_m/σ_{mis}. For both the unmodified and thiokol-modified adhesives, an increase in the stress triaxiality parameter leads to alternating the fracture mode from ductile to brittle and of the yield and rupture criteria from the Mises equivalent stress to the maximum principal stress.

For the rubber modified adhesive, yield behavior was observed irrespective of the scarf angle as in Fig. 12. However, yield criterion alters from the Mises equivalent stress to the maximum principal stress with increasing of the stress triaxiality parameter. The former and latter results imply that shear yielding and damage yielding occur in the adhesive layer, respectively.

From the above discussion, we concluded that the stress triaxiality parameter is available for estimating yield and fracture stresses, but also grasping the fracture morphology of several kinds of adhesively bonded joints.

4. Conclusions

Yield and fracture criteria of three kinds of adhesives were investigated for adhesively bonded scarf joints, butt joint with thin wall tube and bulk specimens. Stress triaxiality of the joints was widely varied, the main result being obtained as follows.

(1) For adhesive joints bonded by the unmodified adhesive , ductile fracture was observed, and Mises equivalent stress at the yield point is almost constant in the range of $0 \leq \sigma_m/\sigma_{mis} \leq 0.42$. When $\sigma_m/\sigma_{mis} > 0.42$, brittle fracture occurred and the maximum principal stress at the fracture point is almost constant.

(2) For adhesive joints bonded by the Thiokol modified adhesive, Mises equivalent stress at the yield point is almost constant in the range of $0 \leq \sigma_m/\sigma_{mis} \leq 1.23$, and ductile fracture occurred except for the butt joint at $\sigma_m/\sigma_{mis} = 1.62$.

(3) For adhesive joints bonded by the rubber-modified adhesive, yielding behavior was observed even in the butt joint. The yield criteria depend on the stress triaxiality parameter: the Miese equivalent stress at the yield point was almost constant in the range of $0 \leq \sigma_m/\sigma_{mis} \leq 0.47$. The maximum principal stress at the yield point was almost constant for $\sigma_m/\sigma_{mis} > 0.47$. The former and latter results suggest that shear yielding and damage yielding occur in the adhesive layer, respectively.

References

1. N. E. BEKHET and D. C. BARTON, *J. of Mater. Sci.* **29** (1994) 4953.
2. M. KAWAGOE and M. KITAGAWA, *ibid.* **23** (1988) 3927.
3. R. H. SIGLEY, A. S. WRONSKI and T. V. PARRY, *ibid.* **26** (1991) 3985.
4. A. SILVESTRE, A. RAYA, M. FERNANDEZ-FAIREN, A. ANGLADA and J. A. PLANELL, *ibid.* **25** (1990) 1050.
5. M. IMANAKA and T. IWATA, *J. of Adhesion* **59** (1996) 111.
6. J. L. LUBKIN, *Trans. ASME, J. of Appl. Mech.* **24** (1957) 255.
7. Y. SUZUKI, *Bulletin of JSME* **27** (1984) 2372.
8. *Idem., ibid.* **28** (1985) 2575.
9. *Idem., JSME Inter. J.* **30** (1987) 1042.
10. R. D. ADAMS and W. C. WAKE, "Structural Adhesive Joints in Engineering" (Elsevier Applied Science Publishers, 1986) p. 125.
11. R. G. BUDYNAS, "Advanced Strength and Applied Stress Analysis" (McGraw-Hill, 1977) p. 362.
12. K. NOUNO and T. NAGAHIRO, *J. of Adhesion Soc. of Japan* **22** (1993) 3 (in Japanese).
13. K. HASHIMOTO, "Epoxy Resins" (Nikkan-kogyo-shinn-bunnsha, 1978) p. 95 (in Japanese).
14. A. K. KINLOCH, in "Structural Adhesives: Developments in Resins and Primers," edited by A. K. Kinloch (Elsevier Applied Science, 1986) p. 127.
15. I. M. WARD and D. W. HARDLE, "An Introduction to the Mechanical Properties of Solid Polymers" (John Wiley & Sons Ltd., 1993) p. 221.
16. W. J. CANTWELL and A. C. ROULIN-MOLONEY, in "Fractograph and Failure Mechanisms of Polymers and Composites," edited by A. C. Roulin-Moloney (Elsevier Applied Science Publisher, 1988) p. 387.
17. A. Y. YEE, *J. of Mat. Sci.* **28** (1993) 6392.
18. ASM Handbook Committee, "Metals Handbook, Vol. 9: Fractograph and Atlas of Fractogtaphy," 8th ed. (American Society for Metals, 1974) p. 91.
19. G. DOLEV and O. ISHAI, *J. of Adhesion* **12** (1981) 283.
20. JEAN LEMAITRE, "A Course on Damage Mechanics" (Springer Verlag, 1992) p. 44.

Received 30 March
and accepted 22 November 1999